

Article

Not peer-reviewed version

---

# Effect of Combined Addition of CeLa and GdY on Microstructure and Mechanical Properties of As-Cast Al-Cu-Mn Alloys

---

Haiyang Zhang , [Mingdong Wu](#) , Zeyu Li , Yang Huang , [Daihong Xiao](#) \* , Lanping Huang , [Wensheng Liu](#)

Posted Date: 13 November 2023

doi: 10.20944/preprints202311.0815.v1

Keywords: Al-Cu-Mn casting alloy; Rare earth micro-alloying; Microstructure; Mechanical properties



Preprints.org is a free multidiscipline platform providing preprint service that is dedicated to making early versions of research outputs permanently available and citable. Preprints posted at Preprints.org appear in Web of Science, Crossref, Google Scholar, Scilit, Europe PMC.

Copyright: This is an open access article distributed under the Creative Commons Attribution License which permits unrestricted use, distribution, and reproduction in any medium, provided the original work is properly cited.

Disclaimer/Publisher's Note: The statements, opinions, and data contained in all publications are solely those of the individual author(s) and contributor(s) and not of MDPI and/or the editor(s). MDPI and/or the editor(s) disclaim responsibility for any injury to people or property resulting from any ideas, methods, instructions, or products referred to in the content.

## Article

# Effect of Combined Addition of CeLa and GdY on Microstructure and Mechanical Properties of as-Cast Al-Cu-Mn Alloys

H.Y. Zhang, M.D. Wu, Z.Y. Li, D.H. Xiao <sup>\*</sup>, Y. Huang, L.P. Huang and W.S. Liu

(National Key Laboratory of Science and Technology on High-strength Structural Materials, Central South University, Changsha 410083, China)

<sup>\*</sup> Correspondence: daihongx@csu.edu.cn; Tel: +86-731-88877880

**Abstracts:** In this study, the effects of combined addition of CeLa and GdY on microstructure and mechanical properties of as-cast Al-4Cu-1Mn alloys were investigated by X-ray diffraction (XRD), scanning electron microscopy (SEM), transmission electron microscopies (TEM) and tensile testing. The results show that the minor addition of CeLa and GdY leads to the refinement of grain size. The addition of CeLa results in the formation of supersaturated vacancies in the Al matrix, whereas the addition of GdY leads to a decrease in the precipitation temperature of the Al<sub>2</sub>Cu phase. The combined CeLa and GdY addition can significantly increase ultimate tensile strength (UTS) while losing only a small amount of elongation (EL). Compared with the unmodified alloy, the grain size and SDAS of the alloy (0.2 wt% CeLa + 0.1 wt% GdY) were diminished by 67.2% and 58.7%, respectively, while maximum hardness and UTS rose by 31.2% and 36.9%, correspondingly.

**Keywords:** Al-Cu-Mn casting alloy; rare earth micro-alloying; microstructure; mechanical properties

## 1. Introduction

Al-Cu-Mn alloys have been extensively used in military and automotive applications due to their high strength, good corrosion resistance and excellent fatigue properties [1,2]. In the preparation of materials, we constantly strive for high overall performance. Unlike deformable aluminum alloys, the properties of as-cast Al-Cu-Mn alloys are highly dependent on the melting and casting process. During the casting process, casting defects (such as hot crack and shrinkage cavity) are inevitable to form, which limits their widely application. Therefore, improving their castability is particularly important to improve the microstructure and mechanical properties of as-cast Al-Cu-Mn alloys.

Adding small amounts of rare earth (RE) such as Ce [3–5], La [6,7], Sm [8,9], Gd [10–12] and Er [13,14] have been proved as a good role in the purification and densification of aluminum alloy melt, reducing casting defects and making the microstructure more dense [15,16]. At the same time, the addition of RE can refine the grain size of the as-cast alloy by promoting the composition overcooling [17]. Yao et al. found that adding 0.3 wt.% La had a significant refining effect on Al-Cu alloy grains due to its segregated and collected in the solidification front [6]. The addition of RE can also promote the formation of RE-rich phases and improve the comprehensive properties of aluminum alloys [18]. For example, Amer et al. discovered the existence of the Al<sub>8</sub>Cu<sub>4</sub>Gd phase in Al-Cu alloys when 0.25 wt.% Gd was added [10]. These phases improved the mechanical properties of Al-Cu alloys. Guo et al. found that the strength and hardness of the alloys with the addition of 0.1 wt% Y were increased due to the existence of the Al<sub>8</sub>Cu<sub>4</sub>Y phase [19]. The individual RE (Ce [20], La [21], Gd [22] and Y [23]) can all modify Al-Cu-Mn alloys to enhance their overall performance. However, excessive addition of individual RE can lead to coarse grains and excessive intermetallic compounds, which have a detrimental effect on the mechanical properties.

The literatures have reported the effect of the combined addition of CeLa [24,25], LaY [26], CeY [27], LaPr [28] and LaSc [29] on microstructure and properties of Al-Cu alloys. The results show that binary combined additions of Re has a significant effect on the grain refinement of the alloy. Liu et al. [30] studied the impact of 0.3 wt.% LaCe on the solidification process of Al-Cu alloys. Their findings indicated that CeLa could increase melt subcooling by inhibiting the nucleation of  $\alpha$ -Al on large heterogeneous particles, resulting in grain refinement. Furthermore, binary combined additions of Re demonstrated better performances than single additions of rare earth element. Wang et al. found that the simultaneous addition of CeY had a better grain refinement effect than the addition of Ce singularly [27]. Song et al. added La and LaSc to Al-Cu alloys [29]. The results showed that the grain size of Al-Cu-La-Sc alloy (69.25  $\mu\text{m}$ ) was smaller than that of Al-Cu-La alloy (118.53  $\mu\text{m}$ ). However, binary combined additions of RE above a certain amount can also have an adverse effect on the mechanical properties of the alloy. Du et al. [31] investigated the microstructure and mechanical properties of Al-Cu-Mn alloys with different CeLa additions. The results showed that the addition of 0.25 wt.% CeLa improved the room temperature mechanical properties of the alloy, but the addition of 0.5 wt.% CeLa promotes the formation of coarse  $\text{Al}_8\text{Cu}_4\text{Ce}$  and  $\text{Al}_6\text{Cu}_6\text{La}$  phases, resulting in a decrease in mechanical properties.

Based on the above analysis, the multi-compound addition of RE can be used as a potential way to reduce the casting defects of alloys. Furthermore, the multi-compound addition of RE presents the opportunity to achieve highly refined grains and generate a suitable quantity of intermetallic compounds using a lower total amount of RE, resulting in superior mechanical properties. Previous literatures [27,29] have reported the effect of LaSc or LaPr in Al-Cu alloys, respectively. Although the RE (Sc or Pr) has a good modifying effect, the RE has a high price and is not suitable for large-scale application. The storage capacity of RE (Ce, La, Gd, and Y) accounts for the largest proportion of all rare earth elements, and their prices are 80-100 times lower than Sc. Therefore, it would be an interesting research direction to study the effect of combined addition of Ce, La, Gd, and Y on the microstructure and mechanical properties of Al-Cu alloys. However, little research has investigated the effect of combined addition of CeLa and GdY on Al-Cu-Mn alloys.

In the study, the effects of combined additions of CeLa and GdY on the microstructure and mechanical properties of cast Al-Cu-Mn alloys at both room temperature and T6 heat treatment and the relevant mechanisms are clarified. The finds in this study can assist of modifiers and broaden the application of Al-Cu-Mn alloys.

## 2. Materials and Methods

The Al-4Cu-1Mn(wt.%) based alloy was obtained by melting pure Al (purity 99.99 %), Al-Cu, and Al-Mn intermediate alloys in the resistance melting furnace. The Al-4Cu-1Mn alloy was completely melted at 780 °C and then held for 10 min, and predetermined amounts of Al-CeLa and Al-GdY master alloys were wrapped in aluminum foil and added to the molten liquid. The melt was held at 760 °C for 20 min, and when the intermediate alloy was completely melted, the whole melt was refined with  $\text{C}_2\text{Cl}_6$ . Then the melt was stirred briefly and kept warm for 10 min. It was then poured into an uncovered cylindrical steel mould with the dimension of  $\varphi 120 \times 200$  mm (preheated at 250 °C). Finally, the Al-4Cu-1Mn alloy ingots were obtained with composite additions of CeLa and GdY in various compositions. The alloys were subjected to Inductively Coupled Plasma Atomic Emission Spectrometry (ICP-AES) analysis to determine their chemical composition and the results are shown in Table 1.

**Table 1.** Normal compositions of the experimental alloys (wt.%).

Alloys	Cu	Mn	CeLa	GdY	Al
Alloy 1	4.0	1.05	0	0	Balance
Alloy 2	4.0	1.05	0.20	0	Balance
Alloy 3	4.0	1.05	0	0.10	Balance
Alloy 4	4.0	1.05	0.20	0.10	Balance

The physical phase composition of the alloy was determined by X-ray diffractometry (XRD) and the data obtained were analyzed using jade6.5 software. The T6 heat treatment temperature of the as-cast alloy was determined by Differential Scanning Calorimetry (DSC) analysis with a specimen weight of 10 mg and a temperature increase rate of 10 °C/min. The peak aging state was determined by determining the Vickers hardness using a 200HV-5 hardness tester with a load of 5 kg and a duration of 15 s. The average of five points was taken. The room temperature tensile properties of the alloy were measured using the Instron 3369 testing machine at a loading rate of 2.0 mm/min after the alloy was subjected to a T6 heat treatment (solid solution treatment at 535 °C for 16 h and aging at 180 °C for 6 h). The dimensions of the standard tensile specimen are shown in Figure 1. Ultimate Tensile Strength (UTS), Yield Strength (YS), and Elongation (EL) are determined based on the average of three tests. The micro-morphology was characterized by Optical Microscope (OM), Scanning Electron Microscopy (SEM) equipped with electron backscatter diffraction (EBSD) and Transmission Electron Microscopy (TEM) equipped with energy dispersive spectroscopy (EDS). Aztec Crystal and Image Pro Plus 6.0 software were used to determine the specimen grain size and secondary dendrite arm spacing (SDAS). After the tensile test, the fracture was observed with a scanning electron microscope to determine the possible fracture mechanism of the alloy.

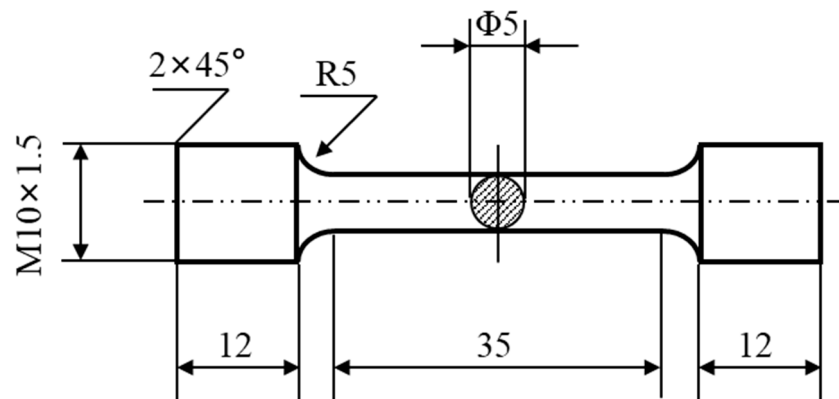


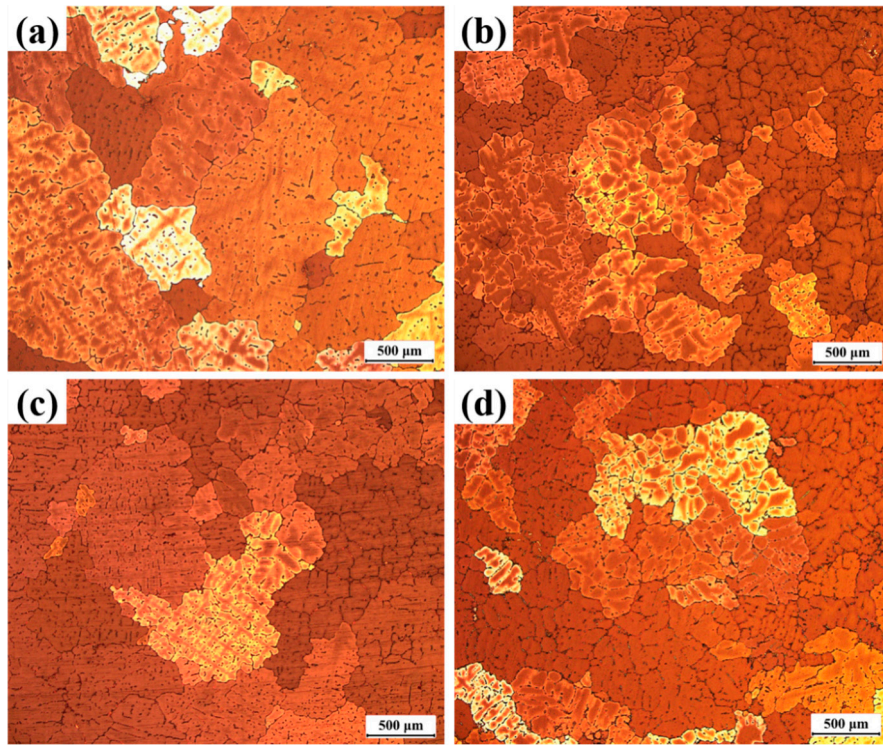
**Figure 1.** Dimensions of standard tensile specimen of the experimental alloy (Unit: mm).

### 3. Results

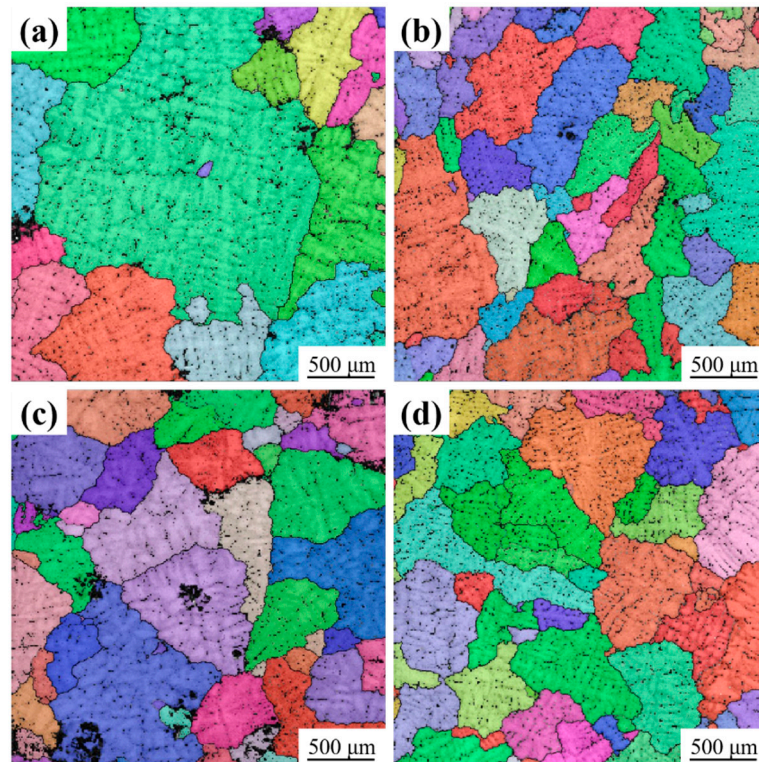
#### 3.1. Microstructure

Figure 2 shows the grain structure corresponding to alloys with different rare earth contents. Compared with the coarse dendrites in the unalloyed Al-4Cu-1Mn alloy (Figure 2a), a significant decrease in the coarse  $\alpha$ -Al dendrites and an increase in the fine isometric  $\alpha$ -Al dendrites in the alloys with the addition of CeLa and GdY, respectively. The grains in the alloys containing CeLa and GdY are predominantly made up of fine equiaxial  $\alpha$ -Al dendrites.

Figure 3 shows the grain size of the studied alloy. Comparison of grain sizes in alloys with varying RE contents indicates a significant decrease in grain size when RE is added. The grain size and SDAS of the alloy were measured using Aztec Crystal and IPP software, as shown in Figure 4. The results show that the grain size and SDAS of the alloy with CeLa and GdY added are reduced from 1022  $\mu$ m and 103.75  $\mu$ m to 386  $\mu$ m and 42.8  $\mu$ m, respectively, as compared to the unalloyed alloy. This suggests that combined addition of 0.2 CeLa and 0.1 GdY (Figure 3d) may provide better refinement than adding 0.2 CeLa or 0.1 GdY (Figure 3b and 3c).



**Figure 2.** Optical macrographs of as-cast Al-4Cu-1Mn alloys (a) Alloy 1, (b) Alloy 2 (0.2 CeLa), (c) Alloy 3 (0.1 GdY) and (d) Alloy 4 (0.2 CeLa + 0.1 GdY).



**Figure 3.** EBSD micrographs of as-cast Al-4Cu-1Mn alloys (a) Alloy 1, (b) Alloy 2 (0.2 CeLa), (c) Alloy 3 (0.1 GdY) and (d) Alloy 4 (0.2 CeLa + 0.1 GdY).

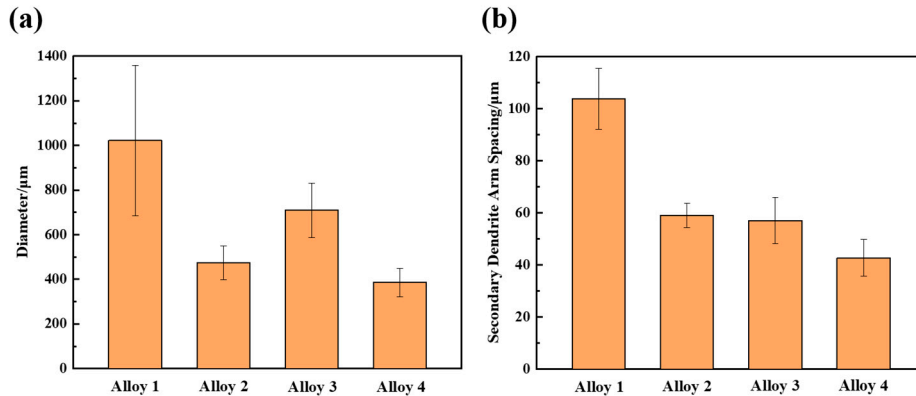


**Figure 4.** Average grain size (a) and SDAS (b) of the as-cast Al-4Cu-1Mn alloys.

Figure 5(a) shows the XRD pattern of combined addition of different RE cast alloys. It can be seen that the alloy 1 without added RE and alloy 2 with added 0.2 LaCe are mainly composed of  $\alpha$ -Al phase and Al<sub>2</sub>Cu phase. However, a small amount of AlCuMnRE phase is detected in the alloy 3 after the addition of GdY. When CeLa+GdY is added, a new phase AlCuRE phase appears in the alloy 4, which may be Al<sub>8</sub>Cu<sub>4</sub>Re phase. Figure 5(b) shows the DSC curves of the studied alloys, which are selected in the temperature range of 380 to 580 °C. It is observed that a heat absorption peak is observed in this temperature interval, which is the melt heat absorption peak of the Al<sub>2</sub>Cu phase. In addition, the peak heat absorption of the alloy 1 without RE addition is 549.9 °C, which is reduced by the addition of GdY. The combined added CeLa+GdY alloy 4 has the smallest peak heat absorption of 540.0 °C.

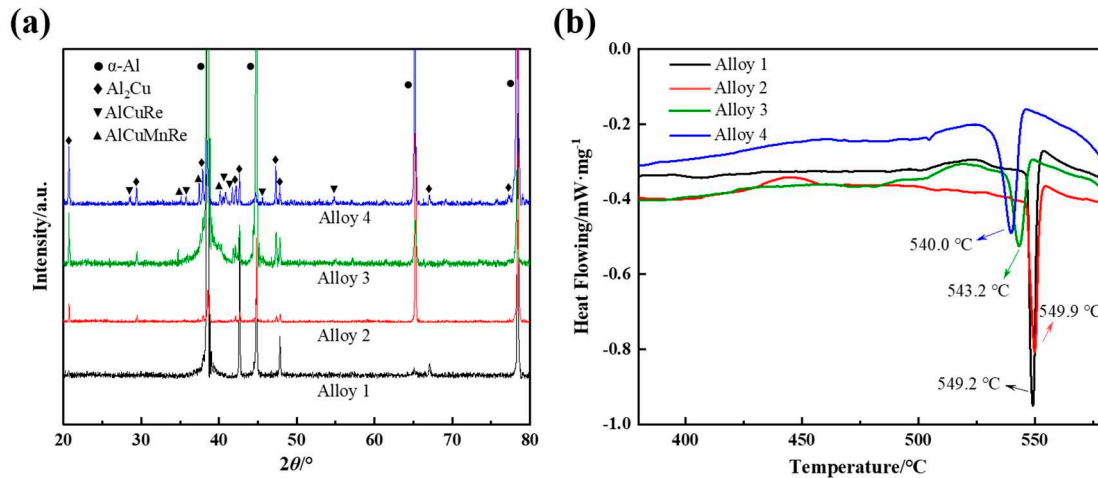


**Figure 5.** XRD patterns (a) and DSC curves (b) of the cast Al-4Cu-1Mn alloys.

Figure 6 shows the backscattered electron (BSE) images of the cast alloys of Al-4Cu-1Mn with varying RE additions. Most of the intermetallic particles formed in the four alloys are observed to be spherical and elongated Al<sub>2</sub>Cu phases. The structure of the Al<sub>2</sub>Cu phase in Al-4Cu-1Mn alloys without RE addition is reticulated. It is located almost discontinuously in the interstices of the secondary dendrite arms and at the grain boundaries (Figure 6a). The addition of CeLa decreases the number of circular Al<sub>2</sub>Cu phases and increases the number of elongated Al<sub>2</sub>Cu phases in the alloy 2, which are connected to each other to form a network. Further magnification reveals the generation of a grey massive phase around a small amount of Al<sub>2</sub>Cu phase (Figure 6b). After the addition of GdY, as shown in Figure 6c, the volume of the circular Al<sub>2</sub>Cu phase in the alloy 3 decreases significantly, and the number of elongated Al<sub>2</sub>Cu phases becomes finer and connects into a network.

Further magnification shows that the  $\text{Al}_2\text{Cu}$  phase is mostly transformed into grey bulk phases. After the combined addition of CeLa + GdY, the size of the round  $\text{Al}_2\text{Cu}$  phase in the alloy 4 further decreases and the number of elongated  $\text{Al}_2\text{Cu}$  phases further increases to form more networks. Further magnification, it is also observed that the elongated  $\text{Al}_2\text{Cu}$  phase mesh structure disappears and the  $\text{Al}_2\text{Cu}$  phase is almost completely transformed into a grey massive phase, while a new bright bulk phase is generated. Combined with the XRD results, it has been determined that the grey massive phase is  $\text{AlCuMnRE}$  and the bright massive phase is  $\text{AlCuRE}$ .

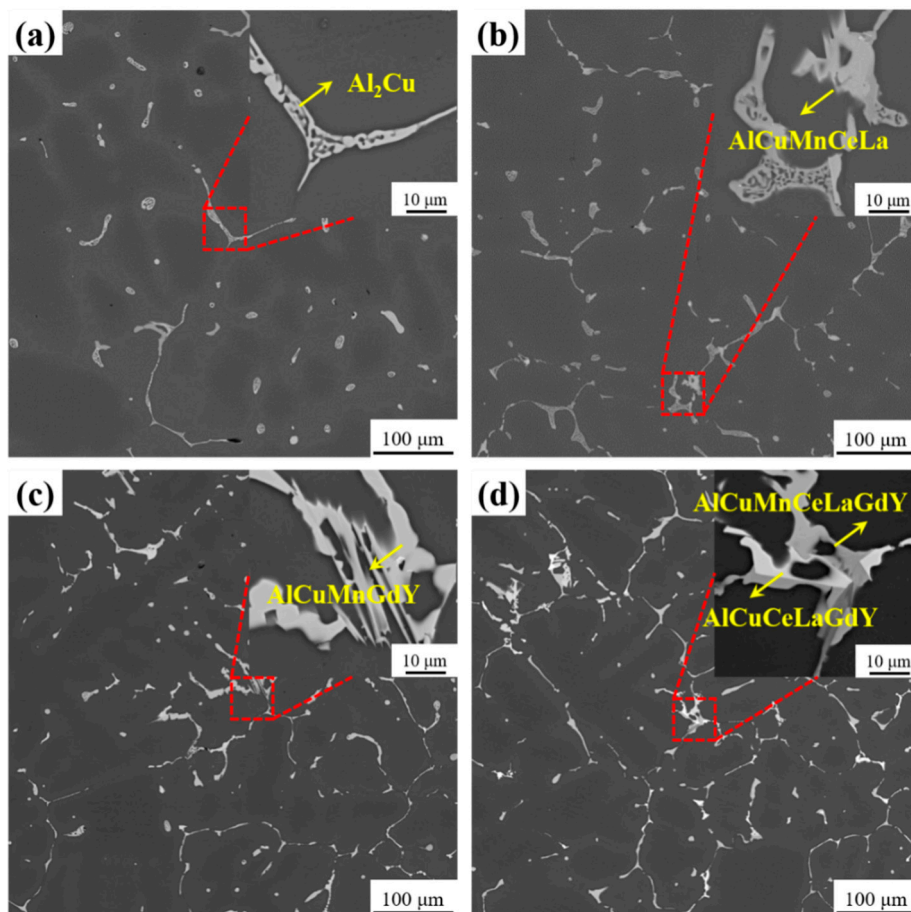


**Figure 6.** SEM images of Al-4Cu-1Mn alloys as cast (a) Alloy 1, (b) Alloy 2 (0.2 CeLa), (c) Alloy 3 (0.1 GdY) and (d) Alloy 4 (0.2 CeLa + 0.1 GdY).

To further investigate the characteristics of intermetallic compounds in alloys after addition of RE. Figure 7 displays SEM images and EDS analyses of the intermetallic compounds of Al-4Cu-1Mn alloys with different RE additions after heat treatment. The bulk grey phase in the unalloyed RE alloy consists of Al, Cu and Mn elements (Figure 7a). With the addition of CeLa, the  $\text{AlCuMnCeLa}$  phase replaces the grey  $\text{AlCuMn}$  phase and a very small amount of bright white  $\text{AlCuCeLa}$  phase is produced (Figure 7b). With the addition of GdY, some grey phases composed of  $\text{AlCuMnGd}$  and white phases composed of  $\text{AlCuMnY}$  are observed (Figure 7c). With the combined addition of CeLa+GdY, the bright white phase of the alloy consists of the elements (Al, Cu, Ce, La, Gd and Y) and the grey phase consists of the elements (Al, Cu, Mn, Ce, La, Gd and Y) (Figure 7d). The findings demonstrate that the combined addition of CeLa+GdY changes the morphology of the RE-rich phases and increases their amount.

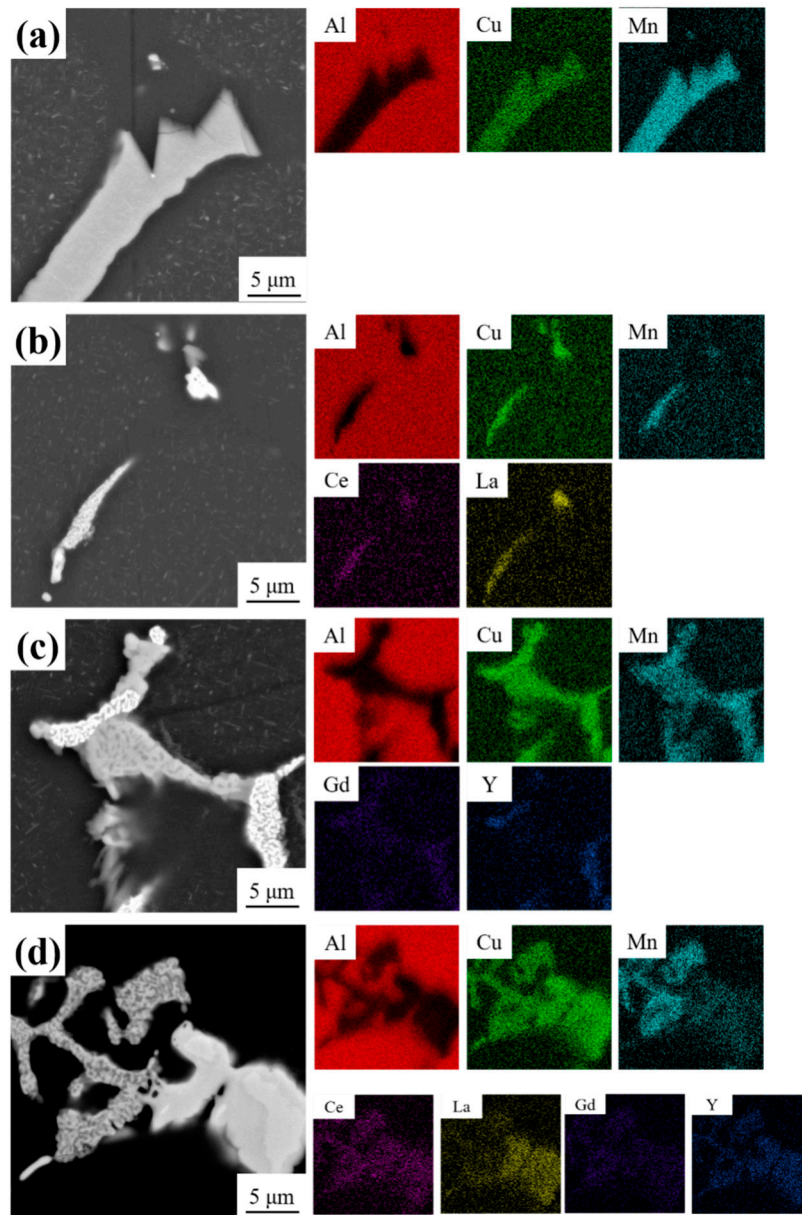


**Figure 7.** SEM morphologies and EDS of the heat-treated Al-4Cu-1Mn alloys (a) Alloy 1, (b) Alloy 2 (0.2 CeLa), (c) Alloy 3 (0.1 GdY) and (d) Alloy 4 (0.2 CeLa + 0.1 GdY).

Figure 8 depicts the TEM images of unalloyed and combined added CeLa and GdY alloys. The short rod-like particles in Figure 8(a)-(c) are  $T(Al_{20}Cu_2Mn_3)$  phase, and the needle-like particles in Figure 8(d) are  $\theta'(Al_2Cu)$  phase. It can be seen that the alloy 1 without the addition of RE contains more coarse T phases and some needle-like  $\theta'$  phases. The quantity of T phases decreases after alloying, especially after the combined addition of CeLa+GdY, the alloy precipitates more  $\theta'$  phases with a more uniform distribution after ageing. Furthermore, observation of the morphology of the  $\theta'$  phase reveals that the addition of CeLaGdY refines the  $\theta'$  phase of the alloy. The results show that the incorporation of CeLaGdY in Al-4Cu-1Mn alloys leads to a reduction in the amount of the T phase and an increase in the volume fraction of the  $\theta'$  phase. In addition, the  $\theta'$  phase exhibits a finer and denser structure.

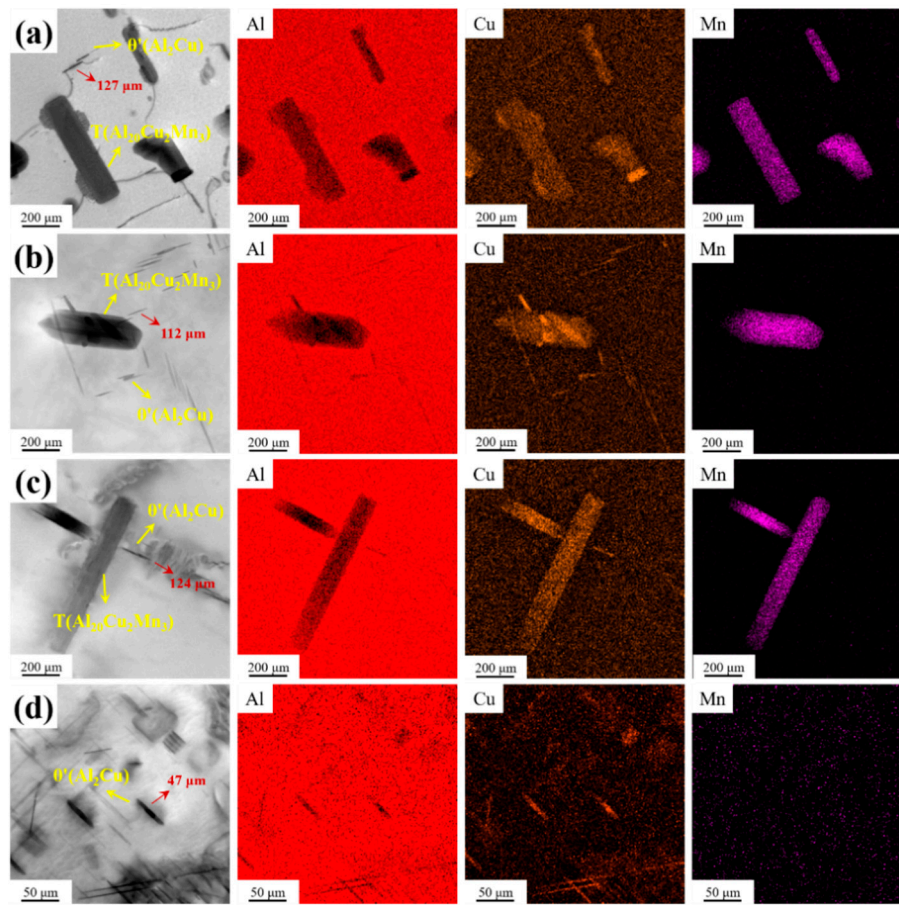


**Figure 8.** TEM images of the heat-treated Al-4Cu-1Mn alloys (a) Alloy 1, (b) Alloy 2 (0.2 CeLa), (c) Alloy 3 (0.1 GdY) and (d) Alloy 4 (0.2 CeLa + 0.1 GdY).

### 3.2. Mechanical Properties

In general, after appropriate heat treatment, cast alloys can only be used as structural materials [32]. Therefore, alloys with different combinations of RE additions were T6 heat treated. The alloy was solid solution treated at 535°C for 16 hours and then aged at 180°C after quenching. Figure 9 shows the ageing curves of the studied alloys. The solid solution heat treatment results in Cu and Mn supersaturation. After quenching, the Al solid solution decomposes into T and θ' phase precipitation and nucleation. Due to the precipitation of strengthening phases, all of the alloys achieved their utmost hardness after being aged at 180 °C for 6 h. Furthermore, it can be seen that the alloy 4 with the combined addition of CeLa and GdY has the highest hardness of 76.5 HV, which is significantly higher than the other three alloys.

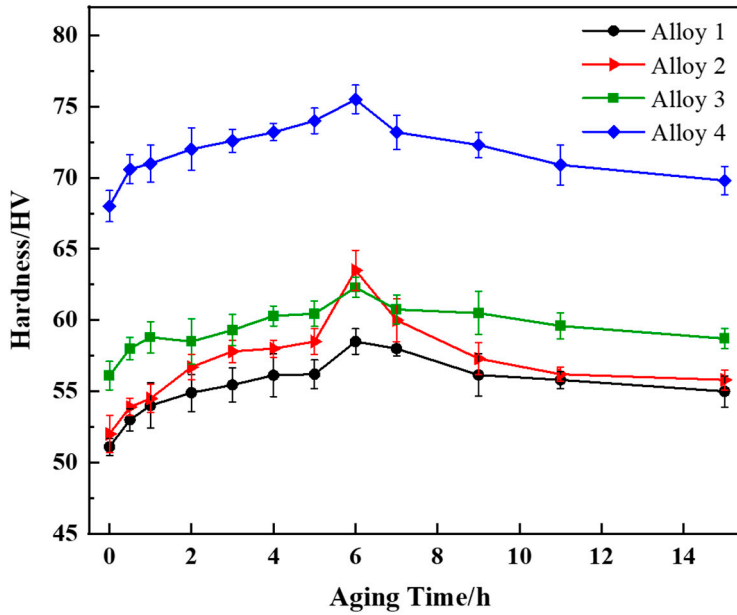


**Figure 9.** Age-hardening curves of Al-4Cu-1Mn alloys with different kinds of RE.

The ultimate tensile strength (UTS), yield strength (YS) and elongation (EL) of various combinations of added RE alloys are shown in Table 2. The unmodified alloy 1 had the lowest values for UTS ( $190.5 \pm 2$  MPa) and YS ( $95.5 \pm 4$  MPa). The addition of CeLa improves the tensile properties of the alloy 2. The addition of GdY increases the tensile strength of the alloy 3 but reduces its elongation. The alloy 4 containing CeLa and GdY exhibits superior performance, increasing UTS by 36.9% compared to the alloy without RE and increasing EL by 17.8% compared to the alloy only containing GdY.

**Table 2.** Results of tensile properties of the heat-treated alloys.

Alloys	UTS (MPa)	YS (MPa)	EL (%)
Alloy 1	$190.5 \pm 2$	$95.5 \pm 3$	$3.71 \pm 0.5$
Alloy 2	$215.8 \pm 3$	$104.5 \pm 4$	$4.27 \pm 0.6$
Alloy 3	$240.8 \pm 2$	$206.9 \pm 3$	$1.29 \pm 0.3$
Alloy 4	$260.9 \pm 4$	$243.7 \pm 2$	$1.52 \pm 0.2$

Figure 10 shows the SEM image of the fracture of the heat-treated tensile specimen. Numerous irregular cleavage planes and holes are distributed at the fracture of the unalloyed RE alloy, as shown in Figure 10(a), indicating that the fracture mode of the alloys is mainly brittle fracture. When unmodified, coarse phases in the alloy 1 are clearly distributed on the fracture surface and some cracks appear on the phase surface. These coarse phases act as a source of cracking and greatly reduce the mechanical properties of the alloy. Furthermore, crack initiation and extension predominantly occur along the interface between the coarse phase and the aluminum base. The adjacent cracks are interconnected, leading to material fracture. Figure 10(b) illustrates a reduction in the quantity of cleavage planes and tearing ridges and an increase in the quantity of dimples in the alloy 2, due to the addition of 0.2 wt% CeLa. When 0.1 wt% GdY is added, the number of dimples in the alloy 3 decreases and their depth becomes shallower, as illustrated in Figure 10(c). Figure 10(d) shows that the combined addition of CeLa and GdY leads to an increase in the number of large tough nests and the presence of particles with cracks at the bottom of the tough nests, which are mainly composed of AlCuMnRE. The fracture mode of the alloy 4 is a combination of brittle fracture and ductile fracture.

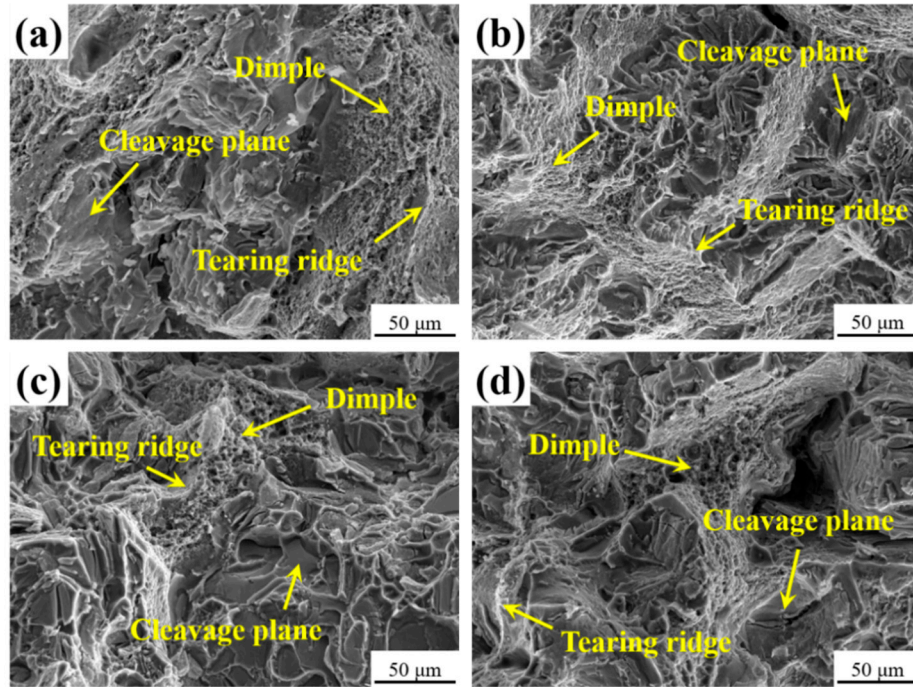


**Figure 10.** Tensile fracture morphologies of the heat-treated Al-4Cu-1Mn alloys (a) Alloy 1, (b) Alloy 2 (0.2 CeLa), (c) Alloy 3 (0.1 GdY) and (d) Alloy 4 (0.2 CeLa + 0.1 GdY).

#### 4. Discussion

Based on the results presented, the addition of RE can refine the grain, increase the number of intermetallic compounds and form new RE-rich phases; at the same time, it can change the size and number of the main hardening phase  $\theta'$  phase and improve the mechanical properties of the alloys. More specifically, the combined addition of CeLa and GdY provides a better grain refinement effect than the separate addition of CeLa or GdY. The larger radius of Ce and La atoms, compared to Al atoms, leads to greater lattice distortions as Ce and La atoms enter the  $\alpha$ (Al) phase, increasing the energy of the whole system. Therefore, CeLa is not effectively dissolved in the  $\alpha$  phase, but is enriched at grain boundaries, leading to an increase in the concentration gradient at the interfacial front, resulting in compositional supercooling and reduction of grain size and SADS. The limited solubility of GdY in the  $\alpha$ -phase causes to aggregate around said phase, resulting in lower liquid-solid surface tension. As a consequence, the supercooling of the solid-liquid interface components is increased and grain refinement is further enhanced.

The combined addition of CeLa and GdY resulted in a significant increase in the number of intermetallic compounds in the alloy 4 and the formation of a new RE-rich phase. This is due to the limited solubility of GdY in the aluminium matrix, which causes them to solidify at the solid-liquid interface and prevents the diffusion of the alloying elements (Cu and Mn) [15]. Simultaneously, RE and alloying elements form  $\text{AlCuMnRE}$  and  $\text{AlCuRE}$  phases along the grain boundaries, which interconnect to form a network, and the alloying elements are consumed in large quantities, leading to a reduction in the volume of the  $\text{Al}_2\text{Cu}$  phase and a change in the microstructure of the alloy.

The combined addition of CeLaGdY resulted in a smaller size and a higher amount of  $\theta'$  phase in the alloy. When CeLa atoms enter the Al matrix, they induce severe lattice distortions, thus increase system energy. To sustain a low energy system, more oversaturated vacancies may aggregate around CeLa atoms. Because of their high binding energy of vacancies, CeLa atom is much easier to migrate and provide the nucleation sites for the formation of  $\theta'$  phase [21]. This leads to an increase in the  $\theta'$  phase density. Meanwhile, the addition of GdY reduces the precipitation temperature of the  $\theta'$  phase (Figure 5b), enhances its nucleation density, and simultaneously lowers the diffusion rate of the alloying element Cu, leading to a delayed coarsening of the  $\theta'$  phase [33].

After heat treatment, a part of the RE dissolves into the Al matrix, filling defects and fully diffusing, eliminating casting defects such as shrinkage holes and microscopic segregation in the alloy, thus improving the mechanical properties of the alloy [34]. The micropores are filled with diffused solute atoms and bonded together. This results in a higher relative density of the alloy and a propensity for the secondary phase to be distributed closely with the matrix grains. Under external stress, the matrix separates from the secondary phase, leading to plastic deformation and formation of tough nests. When CeLa is added alone, the alloy grain size decreases and the refined grains with more boundaries hinder crack extension. The grain refinement strengthening improves the mechanical properties of the alloy. When GdY is added alone, the reticulated AlCuMnGdY phases formed along the grain boundaries in the alloy pin the grain boundaries and form high density dislocation zones that hinder dislocation movement. Dispersion strengthening enhances the alloy strength. Nonetheless, the compatibility for deformation among grains reduces, and the fracture toughness also declines. The combined addition of CeLa+GdY leads to enhanced grain refinement strengthening and dispersion strengthening, significantly increasing the strength of the alloys while improving their plasticity. Simultaneously, the addition of RE improves the nucleation density of the  $\theta'$  phase and retards the coarsening of the  $\theta'$  phase. A large amount of fine diffused  $\theta'$  phases precipitated from the Al matrix after heat treatment, and the precipitation strengthening effect further improved the mechanical properties of the alloy. For these reasons, the fracture mode of the alloy is altered from brittle fracture partially to ductile fracture.

## 5. Conclusions

In this paper, the effect of combined addition of CeLa and GdY on the microstructure and mechanical properties of Al-4Cu-1Mn casting alloy was investigated. Based on the obtained experimental results, the conclusions are as follows:

- (1) The incorporation of 0.2 wt.% CeLa + 0.1 wt.% GdY into the alloy results in sufficient refinement of the  $\alpha$ -Al grains, which changes from dendrites to equiaxed crystals. The volume of Al<sub>2</sub>Cu phase diminishes while the amount of RE-containing phase increases. The average grain size and SADS of  $\alpha$ -Al reduce from 1135  $\mu$ m and 103.75  $\mu$ m to 372  $\mu$ m and 42.8  $\mu$ m, respectively.
- (2) After the combined addition of 0.2 wt% CeLa + 0.1 wt% GdY, the alloy exhibits a bright white AlCuRE phase and a grey AlCuMnRE phase. The secondary phases are closely connected to the matrix grains. The inclusion of RE decreases the precipitation temperature of the  $\theta'$  phase, leading the matrix to precipitate numerous finely dispersed  $\theta'$  phases. The alloy has excellent overall mechanical properties. The average of UTS, YS and EL of the alloy were measured to be 260.9 MPa, 243.7 MPa and 1.52 % respectively.

**Data Availability Statement:** The raw/processed data required to reproduce these findings cannot be shared at this time as the data also forms part of an ongoing study.

**Acknowledgments:** This work was supported by Pre-research Fund (No. 6142912180105).

## References

1. MICHIRI A, SISCO K, BAHL S, et al. A creep-resistant additively manufactured Al-Ce-Ni-Mn alloy [J]. *Acta Materialia*, 2022, 227.
2. DAR S M, LIAO H, XU A. Effect of Cu and Mn content on solidification microstructure, T-phase formation and mechanical property of Al Cu Mn alloys [J]. *Journal of Alloys and Compounds*, 2019, 774: 758-67.
3. WANG J, YANG Z, MA Z, et al. Effect of the addition of cerium on the microstructure evolution and thermal expansion properties of cast Al-Cu-Fe alloy [J]. *Materials Research Express*, 2021, 8(3).
4. TIAN W, HU M, CHEN X, et al. Effect of Ce addition on microstructure, mechanical properties and corrosion behavior of Al-Cu-Mn-Mg-Fe alloy [J]. *Materials Research Express*, 2020, 7(3).
5. YU X, DAI H, LI Z, et al. Improved Recrystallization Resistance of Al-Cu-Li-Zr Alloy through Ce Addition [J]. *Metals*, 2018, 8(12).
6. YAO D, QIU F, JIANG Q, et al. Effect of Lanthanum on Grain Refinement of Casting Aluminum-Copper Alloy [J]. *International Journal of Metalcasting*, 2013, 7(1): 49-54.

7. MAHMOUD M G, SAMUEL A M, DOTY H W, et al. Effect of the Addition of La and Ce on the Solidification Behavior of Al–Cu and Al–Si–Cu Cast Alloys [J]. *International Journal of Metalcasting*, 2019, 14(1): 191-206.
8. RAVANDI S, MARDARE C C, ZENGER T, et al. Samarium influence on current induced atomic displacement in Aluminium and Copper combinatorial thin film alloys [J]. *Thin Solid Films*, 2020, 702.
9. GUO Y, WANG Y, CHEN H, et al. First-principles study on stability, electronic, mechanical and thermodynamic properties of Al–Cu–RE ternary compounds [J]. *Solid State Communications*, 2019, 287: 63-7.
10. AMER S, BARKOV R, POZDNIakov A. Microstructure and Mechanical Properties of Novel Quasibinary Al–Cu–Yb and Al–Cu–Gd Alloys [J]. *Metals*, 2021, 11(3).
11. ZHANG L G, DONG H Q, HUANG G X, et al. Thermodynamic assessment of the Al–Cu–Gd system [J]. *Calphad*, 2009, 33(4): 664-72.
12. ZHANG H, LIU Y, FAN T. Three-Dimensional Network Structure and Mechanical Properties of Al–Cu–Ni–Fe Cast Alloys with Gd Micro-addition [J]. *Metallurgical and Materials Transactions A*, 2021, 52(6): 2613-29.
13. XIE H, ZHAO J, CAO J, et al. Effect of Minor Er Additions on the Microstructures and Mechanical Properties of Cast Al–Cu–Mg–Ag Alloys [J]. *Materials*, 2021, 14(15).
14. AMER S, YAKOVTSYeva O, LOGINOVA I, et al. The Phase Composition and Mechanical Properties of the Novel Precipitation-Strengthening Al–Cu–Er–Mn–Zr Alloy [J]. *Applied Sciences*, 2020, 10(15).
15. FAN L, HAO Q-T, HAN W-K. Dual characteristic of trace rare earth elements in a commercial casting Al–Cu–X alloy [J]. *Rare Metals*, 2014, 34(5): 308-13.
16. CZERWINSKI F. Cerium in aluminum alloys [J]. *Journal of Materials Science*, 2020, 55(1): 24-72.
17. CHEN Z, CHEN P, LI S. Effect of Ce addition on microstructure of Al<sub>20</sub>Cu<sub>2</sub>Mn<sub>3</sub> twin phase in an Al–Cu–Mn casting alloy [J]. *Materials Science and Engineering: A*, 2012, 532: 606-9.
18. XINXIANG Y, DENGFENG Y, ZHIMING Y. Effects of Cerium and Zirconium Microalloying Addition on the Microstructures and Tensile Properties of Novel Al–Cu–Li Alloys [J]. *Rare Metal Materials and Engineering*, 2016, 45(8): 1917-23.
19. GUO T-B, ZHANG F, DING W-W, et al. Effect of Micro-scale Y Addition on the Fracture Properties of Al–Cu–Mn Alloy [J]. *Chinese Journal of Mechanical Engineering*, 2018, 31(1).
20. XIAO D H, WANG J N, DING D Y. Effect of minor cerium additions on microstructure and mechanical properties of cast Al–Cu–Mg–Ag alloy [J]. *Materials Science and Technology*, 2013, 20(10): 1237-40.
21. CHEN Z, CHEN P, MA C. Microstructures and mechanical properties of Al–Cu–Mn alloy with La and Sm addition [J]. *Rare Metals*, 2012, 31(4): 332-5.
22. MAMZURINA O I, AMER S M, GLAVATSKIKH M V, et al. Microstructure and Mechanical Properties of Novel Heat Resistant Cast Al–Cu–Yb(Gd)–Mg–Mn–Zr Alloys [J]. *Metals*, 2022, 12(12).
23. GUO T-B, ZHANG F, DING W-W, et al. Effect of Micro-scale Y Addition on the Fracture Properties of Al–Cu–Mn Alloy [J]. *Chinese Journal of Mechanical Engineering*, 2018, 31(1): 79.
24. ZHAO B, ZHAN Y, TANG H. High-temperature properties and microstructural evolution of Al–Cu–Mn–RE (La/Ce) alloy designed through thermodynamic calculation [J]. *Materials Science and Engineering: A*, 2019, 758: 7-18.
25. ZENG H X, YU H Y, ZHOU Q, et al. Clarifying the effects of La and Ce in the grain boundary diffusion sources on sintered NdFeB magnets [J]. *Materials Research Express*, 2019, 6(10).
26. SHUAI L, ZOU X, RAO Y, et al. Synergistic Effects of La and Y on the Microstructure and Mechanical Properties of Cast Al–Si–Cu Alloys [J]. *Materials*, 2022, 15(20).
27. WANG Y, YUE C, SU M, et al. Effect of Ce on Hot Tearing Sensitivity of As-Cast Al–Cu–Mg–Y Alloy [J]. *Journal of Materials Engineering and Performance*, 2022, 31(8): 6349-59.
28. BAI Z, QIU F, LIU Y, et al. Age Hardening and Mechanical Properties of Cast Al–Cu Alloy Modified by La and Pr [J]. *Advanced Engineering Materials*, 2014, 17(2): 143-7.
29. SONG Z-X, LI Y-D, LIU W-J, et al. Effect of La and Sc Co-Addition on the Mechanical Properties and Thermal Conductivity of As-Cast Al-4.8% Cu Alloys [J]. *Metals*, 2021, 11(11).
30. LIU T, DONG Q, FU Y, et al. Effect of addition of La and Ce on solidification behavior of Al–Cu alloys [J]. *Materials Letters*, 2022, 324.
31. DU J, DING D, ZHANG W, et al. CeLa enhanced corrosion resistance of Al–Cu–Mn–Mg–Fe alloy for lithium battery shell [J]. *Applied Surface Science*, 2017, 422: 221-7.

32. ZHANG F, SHI D, HE Z, et al. Precipitated phase characteristics and fracture behaviour of cast Al–Cu–Mn alloy [J]. *Journal of Materials Research and Technology*, 2023, 25: 2815-25.
33. SONG M, XIAO D, ZHANG F. Effect of Ce on the thermal stability of the  $\Omega$  phase in an Al-Cu-Mg-Ag alloy [J]. *Rare Metals*, 2009, 28(2): 156-9.
34. YU X, ZHAO Z, SHI D, et al. Enhanced High-Temperature Mechanical Properties of Al–Cu–Li Alloy through T1 Coarsening Inhibition and Ce-Containing Intermetallic Refinement [J]. *Materials*, 2019, 12(9).

**Disclaimer/Publisher's Note:** The statements, opinions and data contained in all publications are solely those of the individual author(s) and contributor(s) and not of MDPI and/or the editor(s). MDPI and/or the editor(s) disclaim responsibility for any injury to people or property resulting from any ideas, methods, instructions or products referred to in the content.